Square-lattice photonic crystal microcavities for coupling to single InAs quantum dots

K. Hennessy,[a),b)] C. Reese,[a)] A. Badolato,[a)] C. F. Wang,[c)] A. Imamoğlu,[a),c)] P. M. Petroff,[a),d)] and E. Hu[a),d)]
University of California, Santa Barbara, California 93106

G. Jin, S. Shi, and D. W. Prather
Department of Electrical and Computer Engineering, University of Delaware, Newark, Delaware 19716

(Received 3 July 2003; accepted 5 September 2003)

We have observed optical emission from self-assembled InAs/GaAs quantum dots (QDs) embedded within the single-hole-defect, square-lattice (S1) photonic crystal microcavity. Cavities were measured to have quality factors as high as 4000. Finite-difference time-domain (FDTD) calculations were used to determine the specific S1 geometry that is resonant at the center of our ensemble QD spectrum. Extensive, systematic measurements fully confirmed the FDTD simulations and mapped resonant wavelengths as a function of varying lattice constant and hole radius of the photonic crystal structures. [DOI: 10.1063/1.1623319]

Due to their very small mode volumes (V) and ease of fabrication, photonic crystal microcavities (PCMs) formed in a thin semiconductor membrane have attracted attention as candidate devices to observe cavity quantum electrodynamic (CQED) phenomena. However, cavities constructed for these experiments must also possess high quality factors (Q) to achieve high Q/V, a crucial CQED figure of merit. By applying techniques to minimize coupling to radiative modes, PCMs based on a triangular lattice, supporting high Q modes, have been designed and realized.[1–5] We have previously shown high Q resonances in the triangular-lattice H2 PCM fabricated in a GaAs membrane, excited by InAs/GaAs quantum dots (QDs) embedded within the membrane.[6] The H1 resonance, while having a smaller mode volume, had similar Q/V as the H2 due to a low $Q\sim250$, consistent with the symmetry of the mode. More recently, a high Q, nondegenerate, whispering-gallery-like mode (WGM) has been identified in a single-hole-defect PCM based on a square lattice (S1). The properties of this mode have been studied theoretically[7] and experimentally characterized around 1550 nm using quantum wells as an active region.[8] InAs QDs have also been used as an active layer in the square lattice, exciting lasing modes around 1330 nm in two and four coupled-S1 cavities.[9] Our current work describes the coupling of InAs QDs, emitting around 925 nm, to an S1 cavity with a potentially much higher Q/V than exhibited by the H1 cavity and well suited for CQED with a QD since, in contrast to many of the high Q/V triangular PCMs, the electric field maximum in the S1 cavity is located within the semiconductor region, allowing high spatial overlap between cavity mode and QD emitter.

We designed the hole radius r, lattice constant a, and membrane thickness t of our S1 cavities by using three-dimensional finite-difference time-domain (FDTD) simulation results of a GaAs device with $r/a=0.39$, $t/a=0.6$, and $a=300$ nm, surrounded by air. The calculated frequency response in the defect region is shown in Fig. 1. The simulated H_z magnetic field distribution of the mode at 911 nm is shown in inset (a) over the region of the device shown in inset (b), and confirms the lowest-order WGM nature of this resonance. We have fabricated S1 PCMs of similar a, r/a, and t/a in a 180 nm GaAs membrane, suspended in air. The material is grown by molecular-beam epitaxy on a (100) GaAs substrate. The GaAs membrane is grown after a 500 nm sacrificial layer of $Al_{0.7}Ga_{0.3}As$. Five layers, spaced by 20 nm, of self-assembled InAs QDs blue shifted by partial covering,[10] with a density of $\sim2\times10^{10}$ cm^{-2}, are embedded into the membrane. The AlGaAs layer is selectively etched to form the final PC membrane. The cavity pattern is defined by electron-beam lithography (EBL) using a 50 kV JEOL JBX-5DII(U) EBL system. The pattern is transferred into a SiN mask and subsequently into the GaAs by reactive ion etching. A wet etch in HF releases the final membrane structure. Analyses of loss mechanisms in PC membranes suggest that fabrication accuracy is essential to achieve de-

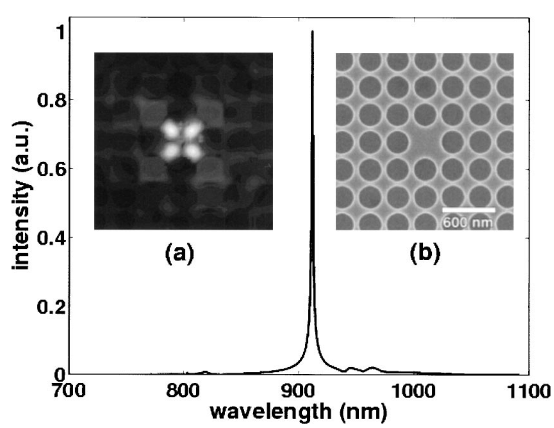

FIG. 1. FDTD calculated frequency response of a cavity with $a=300$ nm and $r/a=0.39$. The simulated H_z field distribution of the mode at 911 nm is shown in inset (a) over the region of the device shown in inset (b).

[a)]Department of Electrical and Computer Engineering.
[b)]Electronic mail: kjh@ece.ucsb.edu
[c)]Department of Physics.
[d)]Materials Department.

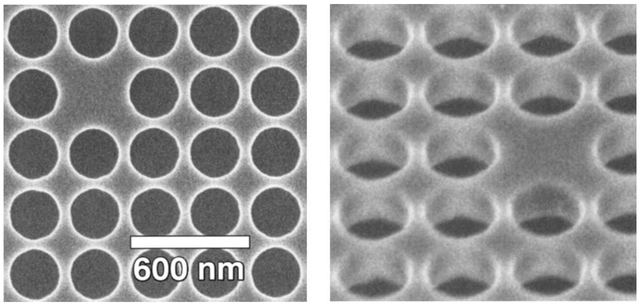

FIG. 2. Scanning electron micrographs of a single-hole-defect PC microcavity with a 300 nm lattice constant, showing a top view (left) and a 45° view (right) of the defect region in a 180-nm-thick GaAs membrane.

sired device performance,[11,12] therefore, we have developed fabrication techniques to minimize variation in hole size across the device and produce PC holes with smooth, straight sidewalls. Details of these techniques are published elsewhere.[13] Scanning electron micrographs of resulting cavities are shown in Fig. 2, where only a few of the ten lattice periods are shown at 0° (left) and 45° (right) views.

Spatially resolved photoluminescence (PL) measurements were performed at 5 K on S1 cavities of varying a and r in order to characterize the WGM spectral location over the entire QD emission range, which is continuous from 880 to 970 nm. Using a diode laser operating in cw at 780 nm, we focused 1.8 kW/cm^2 power density on the sample surface at normal incidence in an estimated 3 μm spot size with a microscope objective (numerical aperture=0.55). Using the QDs to decorate the cavity modes, we collected their emission through the same objective and have observed a single, high Q mode in devices with a between 290 and 310 nm. A sample PL spectrum is shown in Fig. 3 for a PCM of $a=300$ nm and $r/a=0.37$. Cavities with lattice constants between 250–280 and 320–400 nm were tested and determined not to be resonant within our QD emission spectrum. We measured the Q factor of the WGMs by collecting PL with a monochromator having a spectral resolution of 70 μeV and fitting the spectra to Lorentzian functions. Cavities with $a=300$ nm, $r/a=0.38$, and $t/a=0.6$ were of the highest quality, and two spectra of these devices are shown in insets (a) and (b) of Fig. 3, fit to Lorentzians of $Q=4000$ and 3600, respectively. Based on our estimations, the Q value of these cavities is not limited by QD absorption, which we estimate cannot limit Q in the range $Q<10\,000$.

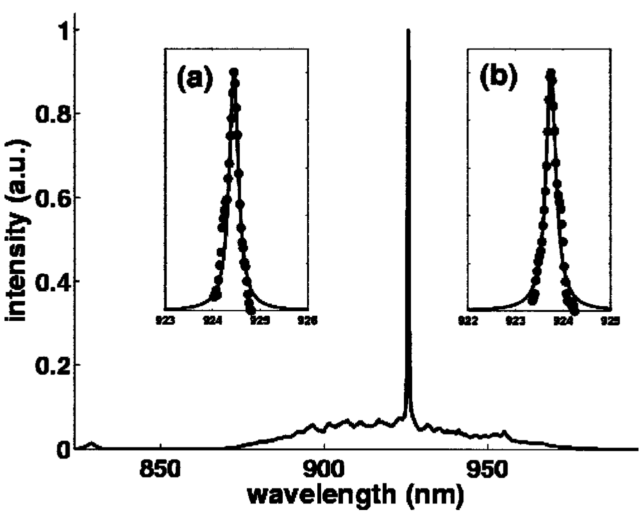

FIG. 3. PL from a typical single-hole-defect, square-lattice microcavity of lattice constant $a=300$ nm and $r/a=0.37$, showing a high Q mode at 926 nm. The InAs QD emission is between 870 and 970 nm. High-resolution PL is displayed in the insets for devices with $a=300$ nm and $r/a=0.38$, fit to Lorentzians of $Q=4000$ (a) and 3600 (b).

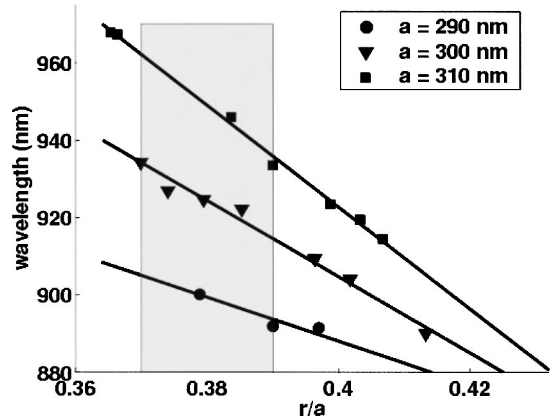

FIG. 4. Wavelength of the whispering gallery mode in a single-hole-defect, square-lattice PC microcavity for various lattice constants, a, as a function of radius divided by a. Modes in the shaded region of the resonant mode map are of highest Q.

We have confirmed the importance of minimizing variation in hole size across the PCMs. Spectra taken on devices with nonuniform r show many closely spaced modes in contrast to the clear, single-mode spectra, as shown in Fig. 3, of devices with uniform r. The additional resonances are defect modes resulting from aperiodic hole r and have been observed in devices with as little as 6% (7.5 nm) decrease in r over ten lattice periods from the center to edge of the PCM. In this letter, all data on WGMs were taken on devices with negligible variation in hole r, therefore exhibiting single-mode spectra.

These cavities incorporated an ensemble of QDs, and it is clearly desirable to locate a single QD at an antinode of the WGM, to achieve strong coupling between the QD and cavity mode. Rather than relying on coincidental spatial and spectral alignment, we would prefer developing a technology to spatially align a PCM around a QD of known emission wavelength, choosing a and r/a to significantly improve the chance of spectral coupling. In such technologies, we must be able to tune the resonant wavelength λ_r of the PCM very precisely, over large ranges, by scaling its geometry. Consequently, utilizing a large set of PCMs fabricated with varying dimensions, we have mapped out three different ways to tune this cavity, each with a different characteristic tuning scale $\Delta\lambda_r$. Large shifts in λ_r, on the order of 25–40 nm, are achieved by changing the lattice constant by $\Delta a=\pm 10$ nm. We achieve moderate tuning of λ_r by about 10 nm by altering r/a in the initial pattern file by $\pm 6\%$, and final, subtle shifts by $\Delta\lambda_r=\pm 1$–2 nm are produced by varying the electron dose in the EBL. We observe a slight increase in r/a when the dose is increased by about 2%, explaining this fine shifting in λ_r. The tuning information is summarized in Fig. 4, which plots S1 resonant wavelength as a function of r/a for three different lattice constants. Each point in this resonant mode map represents the average λ_r of several devices defined with the same pattern in the EBL and has an error bar of about ± 1 nm. Modes in the shaded region of the map are of highest $Q = 2000-4000$. The resonant mode map fully confirms the aforementioned FDTD calculation that predicted a resonance near 911 nm for a device with $r/a = 0.39$ and $a = 300$ nm.

In summary, we have demonstrated the coupling of InAs QDs grown by the partially covered island technique to the WGM of various S1 PCMs. A high density ensemble of QDs with spectral range from 880 to 970 nm was used to characterize the location and quality of the WGMs, revealing resonances with Q as high as 4000. The resonant mode map generated from our measurements, detailing resonant frequency as a function of PCM dimensions, fully confirmed initial FDTD calculations and will be used in techniques aimed to improve the probability of achieving both spatial and spectral coupling of a single QD to a cavity mode for CQED experiments.

The authors thank William Mitchell for assistance with the EBL, the IGERT program of the National Science Foundation for support under award DGE-9987618, AFOSR, and DARPA for grants QUIST MDA 972-01-1-0027 and CNID DMEA 90-02-2-0215.

[1] J. Vučković, M. Lončar, H. Mabuchi, and A. Scherer, Phys. Rev. E **65**, 016608 (2001).
[2] T. Yoshie, J. Vučković, and A. Scherer, Appl. Phys. Lett. **79**, 4289 (2001).
[3] J. M. Geremia, J. Williams, and H. Mabuchi, Phys. Rev. E **66**, 066606 (2002).
[4] J. Vučković, M. Lončar, H. Mabuchi, and A. Scherer, IEEE J. Quantum Electron. **38**, 850 (2002).
[5] J. Vučković and Y. Yamamoto, Appl. Phys. Lett. **82**, 2374 (2003).
[6] C. Reese, B. Gayral, B. D. Gerardot, A. Imamoğlu, P. M. Petroff, and E. Hu, J. Vac. Sci. Technol. B **19**, 2749 (2001).
[7] H.-Y. Ryu, J.-K. Hwang, and Y.-H. Lee, IEEE J. Quantum Electron. **39**, 314 (2003).
[8] H.-Y. Ryu, S.-H. Kim, H.-G. Park, and Y.-H. Lee, J. Appl. Phys. **93**, 831 (2003).
[9] T. Yoshie, O. B. Shchekin, H. Chen, D. G. Deppe, and A. Scherer, Electron. Lett. **38**, 17 (2002).
[10] J. M. García, T. Mankad, P. O. Holtz, P. J. Wellman, and P. M. Petroff, Appl. Phys. Lett. **72**, 3172 (1998).
[11] Y. Tanaka, T. Asano, Y. Akahane, B.-S. Song, and S. Noda, Appl. Phys. Lett. **82**, 1661 (2003).
[12] H.-Y. Ryu, J.-K. Hwang, and Y.-H. Lee, Phys. Rev. B **59**, 5463 (1999).
[13] K. Hennessy, C. Reese, A. Badolato, C. W. Wang, A. Imamoğlu, P. M. Petroff, and E. Hu, J. Vac. Sci. Technol. B (to be published).